SNS ASAC Review September 27-29, 2004

highlights from talks by
S. Henderson, J. Wei, D. Raparia, V. Danilov

Ring Impedance and Instability Update

V. V. Danilov

SNS Oak Ridge, Accelerator Physics

September 27-29, 2004

Talk Motivation and Outline

1) **Response to ASAC recommendations:**
   a) **"…to plot analytical stability diagram, including effect of space charge… it would permit a fast assessment of Landau damping, and it could guide strategies for beam stabilization, e.g. by adjusting chromaticity, nonlinearities, coupling, or the painting scheme. It is an established and fast treatment that would be complimentary to ORBIT simulations"**
   b) **"…the accelerator physicists might want to contemplate whether resistive-wall waves traveling at low velocities could be important for the SNS ring."**
2) **New (improved) measurements for the extraction kicker transverse impedance**

Talk Outline

1) **Only transverse "conventional" instabilities analyzed. Reason – no E-p instability parallel trial runs has just started. For longitudinal instabilities old result still holds – they seem to be important if the number of particles is around $6*10^{14}$ protons (if no parasitic effects from RF system).**
2) **Dominant sources of impedance, which include extraction kicker,**
   resistive wall, and injection kicker coating (including low velocity waves), reexamined and presented in the talk
3) **Coasting beam stability diagrams are analyzed and compared to the simulation**

Colleagues, Collaborators, Advisors

- SNS, ORNL
  - V. Danilov, S. Henderson, J. Holmes, L. Jain (summer student), M. Plum
- BNL
  - M. Blaskiewicz, D. Davino, A. Fedotov, H. Hahn, Y. Y. Lee, J. Wei
- Fermilab
  - A. Burov, V. Lebedev

Resistive Wall and Injection Kicker Impedances

Following ASAC recommendations, we analyzed paper by Karliner, et. al. (EPAC96) that claims that the resistive impedance may strongly depend on velocity of transverse waves.
It could be relevant for the SNS Ring – we have medium relativistic beam, besides slow waves have velocities few times lower than the velocity of light

CALCULATION OF TRANSVERSE RESISTIVE IMPEDANCE
FOR VACUUM CHAMBERS
WITH ARBITRARY CROSS SECTIONS

M.M. Karliner, N.V. Mityanina, D.G.Myakishev, V.P. Yakovlev
Budker Institute for Nuclear Physics, Novosibirsk, Russia

7 CONCLUSION

1. The necessity of taking into account the phase velocity of the current harmonic is shown.

2. The small phase velocity of the dangerous current harmonic is mostly important in the case of the multilayer wall with the vacuum gap between layers, which are thinner than the skin depth. For the vacuum chamber of LHC, it is important in the case of not everywhere copper coating.

3. The most unstable mode of the transverse oscillations of the multibunch beam and the most dangerous frequency should be found with the account of the phase velocities of the current harmonics.

4. The FEM method is developed for the numerical solution of the excitation problem for arbitrary phase velocity of the exciting current harmonic, taking into account both E_z anf H_z field components.

5. One should note that at small phase velocities, the addition due to the transverse components of the current can be sufficient and should not be neglected. In future, this fact should be proved and taken into account.

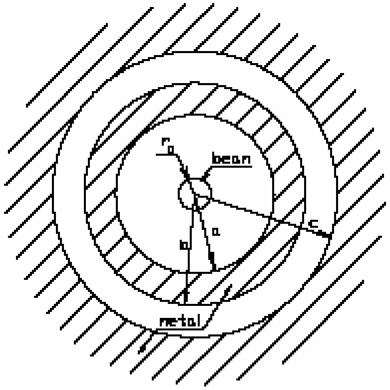

Figure 1: Cross section of the round multilayer tube.

The paper was analyzed by our group and A. Burov (FNAL).
Our conclusion- the results of the paper are not valid.

Burov/Lebedev (BL) vs. M. Karliner et al.

- BL method can be applied for a specific geometry analyzed by M. Karliner et al. (MK) The results are in contradiction.
- First, BL result does not depend on the wave length of the perturbation when its frequency is fixed. According to MK, impedance depends on the wave length.
- Second, for MK limit case of “infinite phase velocity” their impedance goes to a wave length independent asymptotic. However, even in this case BL method applied for this geometry leads to results different from MK.

BL versus MK

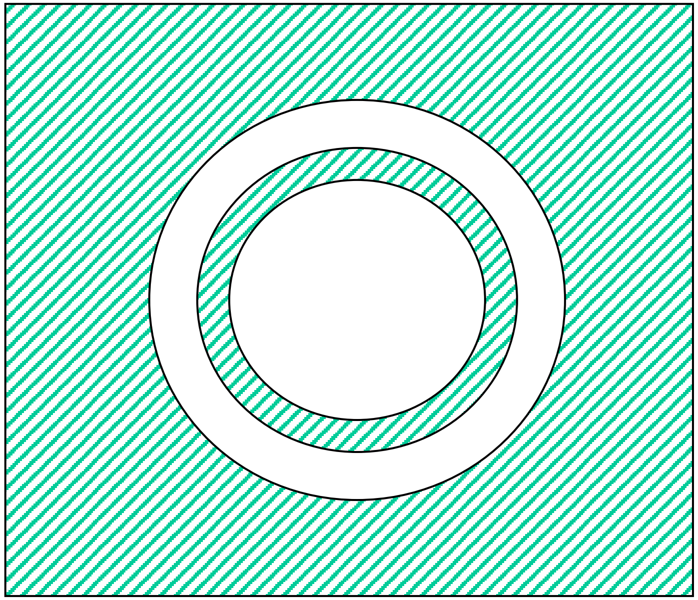

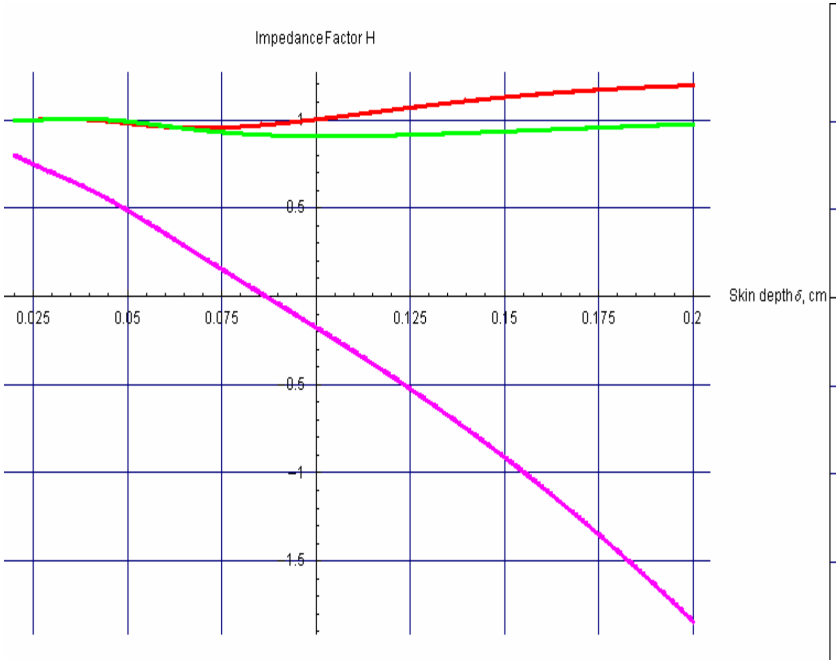

The geometry for the KL paper
Example for resistive wake calculation

Ratio of thick-wall resistive wall impedance and BL impedance (red), MK for high phase velocities (green), and MK for low phase velocities (magenta).

MK vs MK

- A. Burov recently discussed this disagreements with two MK authors, V. Yakovlev and N. Mityanina. He was told that that EPAC'96 MK paper has to be considered as preliminary, the authors do not confirm now their results.
- The first author, M. Karliner, later came to a conclusion that under conventional assumptions the impedance is always independent on the wave length.
- V. Yakovlev explained in private communication that not all the related terms were properly collected in the MK EPAC'96 paper. He expressed his assurance that the correct result must be wave length independent.

Why the Wave Length Can Be Neglected

- In the long wave length limit, the currents and fields induced in the resistive walls of the vacuum chamber, are driven by the oscillating local offset of the beam.
- When the wave length is long compared with the aperture, its actual value is irrelevant for the transverse diffusive dynamics of the induced fields. The electromagnetic fields are determined by diffusion process that is local and doesn't propagate longitudinally.
- This diffusion is determined by the local beam parameters, as the frequency of oscillations, and it knows nothing about beam global values, such as the wave length, as long as it is much larger than the vacuum chamber aperture.
- In this case, there is no dependence of impedance on wavelength and, therefore, on particle and phase velocity, as soon as the frequency is fixed (it is the only parameter of the problem).

Our conclusion – the SNS old resistive impedance estimations are correct.

Injection Kicker Impedance

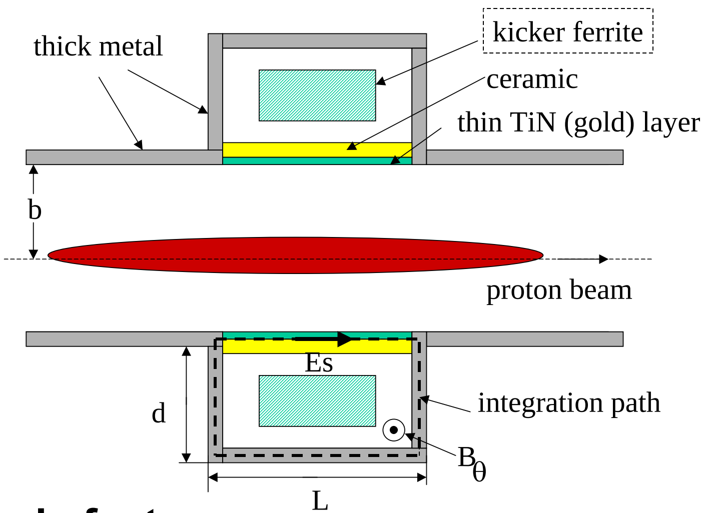

Shown is the model of injection kicker. Yellow layer is ceramic, green is a TiN+Cu layer (resistivity 45 μΩ cm, thickness 18 μm) on the inner surface of the SNS ceramic chambers Inner radius 8 cm, ceramic thickness 1.25 cm and total length of 5m for 8 of them.

Basic facts:

1) **Longitudinal impedance is just resistivity of the TiN layer (the EM fields shielded by surface currents from penetration to ferrite-filled cavity.**
2) **Transverse Impedance could be estimated from Panofsky-Wenzel formula.**

The estimation is $Z_{\perp} = \frac{2c}{\omega b^2} Z_{\|}$ **(*b* is the radius of the chamber,** $Z_{\|} = 0.25\,\Omega$ **)**

3) This result lead to recently discovered closed orbit instability

(SNS Acc. Group, PRST-AB 4, 120101 (2001))

Injection Kicker Transverse Impedance

More accurate estimation (Burov, Lebedev (FNAL)) is shown in Fig. below

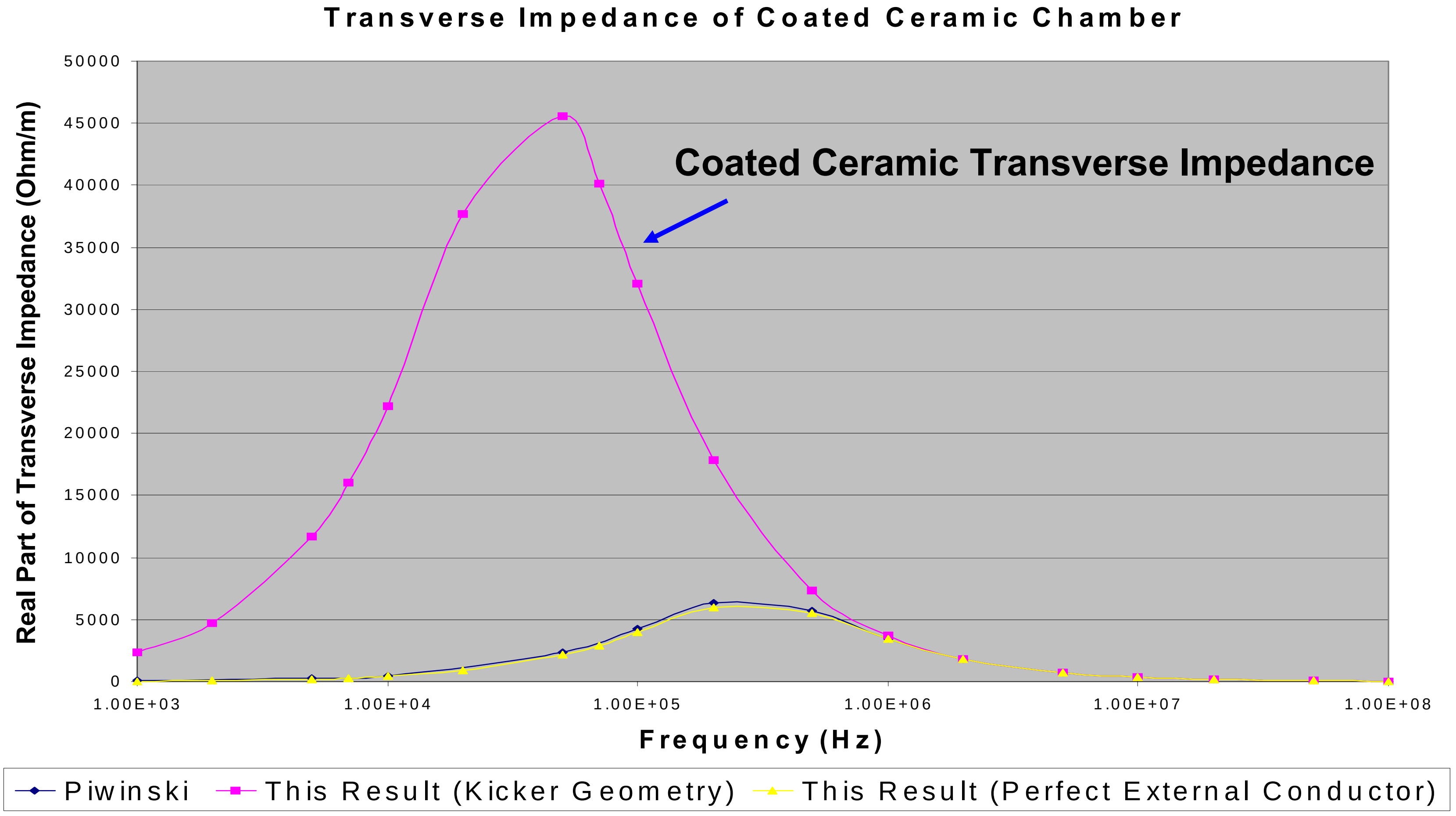

For this result the closed orbit instability threshold moved up to 10^{15} protons in the SNS Ring (the instability is still important for VLHC, SuperB-factory and other high current rings)

Summary of Resistive Wall Instability

- Long Memory Wakes: Resistive Wall & Injection Kicker Coating
  - The beam is stable for baseline working point (6.23, 6.2)
  - Causes instability of the harmonic with the lowest frequency (200 kHz) for the backup working point (6.3, 5.8) – increment is about 200 turns for zero chromaticity. The total real part of the impedance for this frequency was 32 kΩ/m =24(injection kicker)+8 (resistive wall) kΩ/m
  - Natural chromaticity kills the instability
  - Closed orbit instability threshold is 10^{15} protons for improved impedance model
  - Extraction Kicker Impedance and Ep Instability –are biggest concerns for the SNS Ring

Extraction Kicker Updated Transverse Impedance

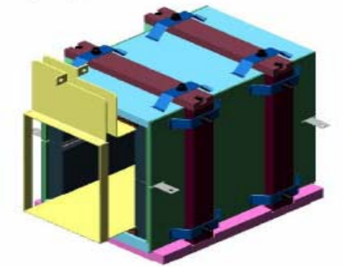

Extraction Kicker RF cavity Impedance (last measurements by H. Hahn)

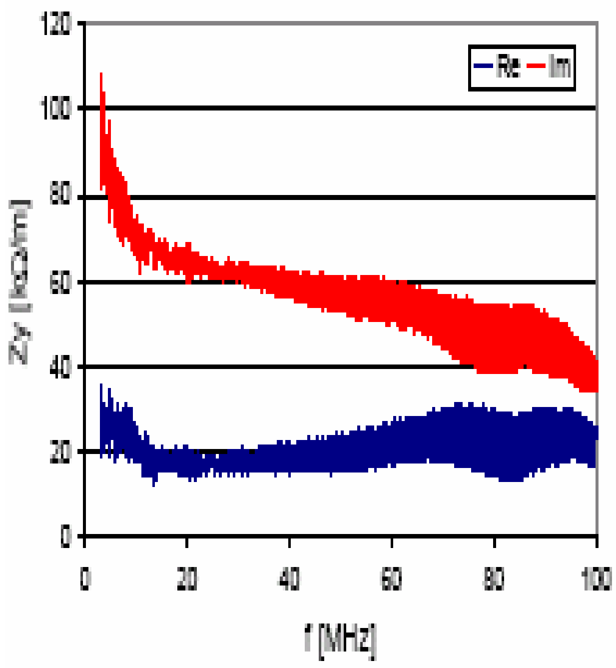

Transverse Impedance with PFN

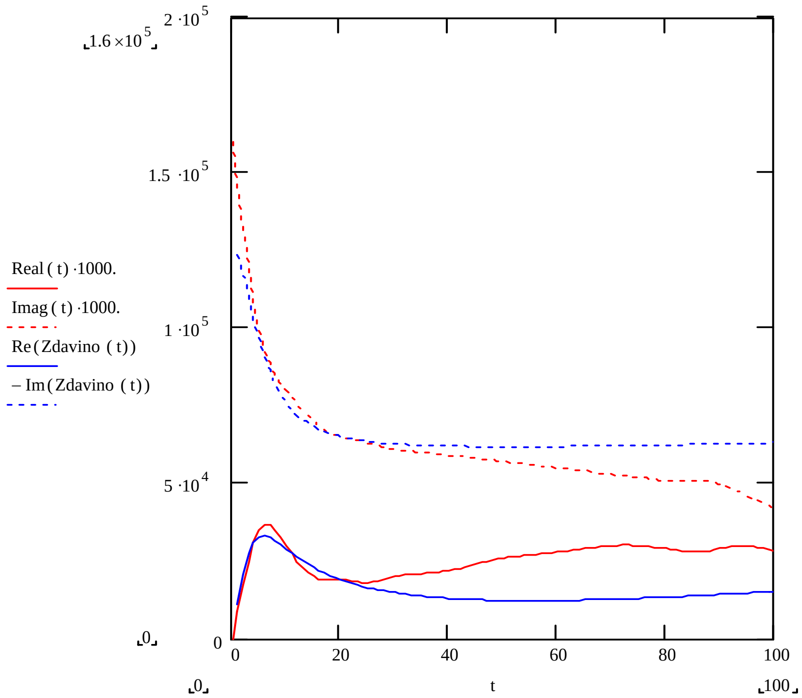

Old results (blue lines) *vs* new data (red lines). Solid lines – real parts, dots – Imaginary parts.

Instability for the Extraction Kicker Impedance

Threshold Estimates are Unchanged from earlier work by Fedotov, *et al*:
$3*10^{14}$ for natural chromaticity and **$2*10^{14}$** for zero chromaticity.
New runs to update these thresholds are underway.

Basic parameters that influence the threshold (except the impedance):

1) Energy spread;
2) Chromaticity;
3) Beta-functions and tunes;
4) Transverse beam distribution.

Is it possible to use simple stability diagrams for coasting beam to comprehend dependencies of the threshold on listed above parameters?

Stability Diagrams (prerequisites)

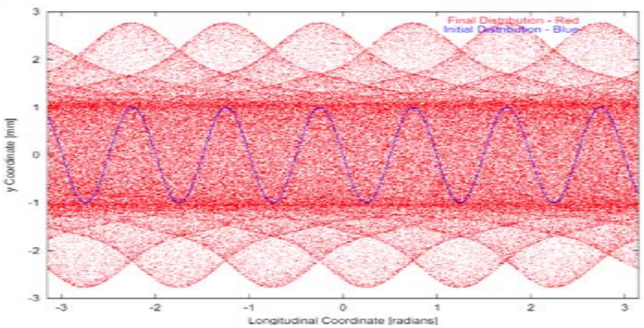

This figure shows typical behavior of average dipole moment (blue) and particle displacements (red) vs longitudinal coordinate for single harmonic. Harmonic number n=6, frequency of beam oscillation at fixed point is $n\omega_0 \pm \omega_b$ (fast and slow waves) plus small corrections due energy offset δ and chromaticity ξ

Newton equation with relativistic mass

$$\frac{d^2 D}{dt^2} + \omega_b^2 D = \frac{F}{\gamma m}$$

the total time derivative has to be rewritten into partial derivatives for moving beam

$$\frac{d}{dt} = \frac{\partial}{\partial t} + \frac{dz}{dt}\frac{\partial}{\partial z} + \frac{d\delta}{dt}\frac{\partial}{\partial \delta}$$

force

$$F = -\mathrm{Re}\{ iqID(z,\delta,\tau) Z_\perp (n\omega_0 + \omega_b)\delta_\Pi (s - s_0)\}$$

dipole moment *D* has fast harmonic oscillation and slow factor d_s that is what needs to be found

$$D(z,\delta,\tau) = d_s(\delta,\tau)\exp\{i(2\pi n\frac{z}{\Pi} + \omega_b t)\} = d_s(\delta,\tau)\exp\{i[2\pi(n+\nu_b)\frac{z}{\Pi} + 2\pi\nu_b\tau]\}$$

after substitution Newton equation yields

$$2i\omega_b\left(\frac{\partial}{\partial t}d_s + \frac{dz}{dt}\frac{\partial}{\partial z}d_s + \frac{d\delta}{dt}\frac{\partial}{\partial\delta}d_s\right) = \frac{F\exp(-i\omega_b t)}{\gamma m}$$

$$\chi = \frac{-qIZ_\perp(n\omega_0 + \omega_b)}{2\gamma m(\beta c)^2}\beta_{s_0}$$

assuming dδ/dt=0 (extraordinary simplification forcoasting beam), one gets

$$\frac{\partial d_s(\delta,\tau)}{\partial\tau} + i\Delta(\delta)d_s(\delta,\tau) = \chi\int_{-\infty}^{\infty} g(\delta)d_s(\delta,\tau)d\delta$$

$$\Delta(\delta) = \frac{\eta\delta}{\beta^2}2\pi\left|n + \nu_b + \xi\right|$$

$$i(\alpha + \Delta(\delta))d_s(\delta) = \chi\int_{-\infty}^{\infty} g(\delta)d_s(\delta)d\delta \rightarrow 1 = \chi\int_{-\infty}^{\infty} g(\delta)\frac{1}{i(\alpha+\Delta(\delta))}d\delta$$

Dispersion Relation

Energy Distributions Considered (courtesy J. Holmes)

- The plots show the energy distributions at the longitudinal density peak at the end of injection for a 1.44 MW case, both without (top plot) and with (bottom plot) the HEBT EC and ES cavities.
  - Red curves are obtained directly from ORBIT,
  - Blue curves are computed fits:
    - Top plot is sum of Heaviside and Gaussian.
    - Bottom plot is sum of Heaviside and rational function:

$$k \times \frac{x^2 + a^2}{x^8 + b^8}$$

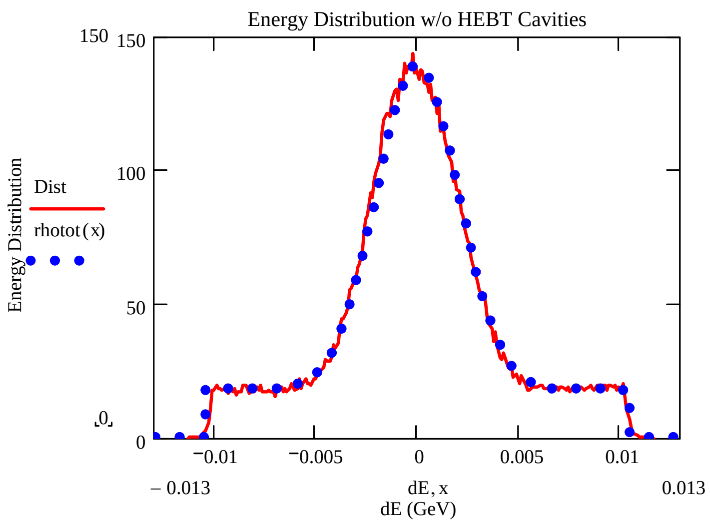

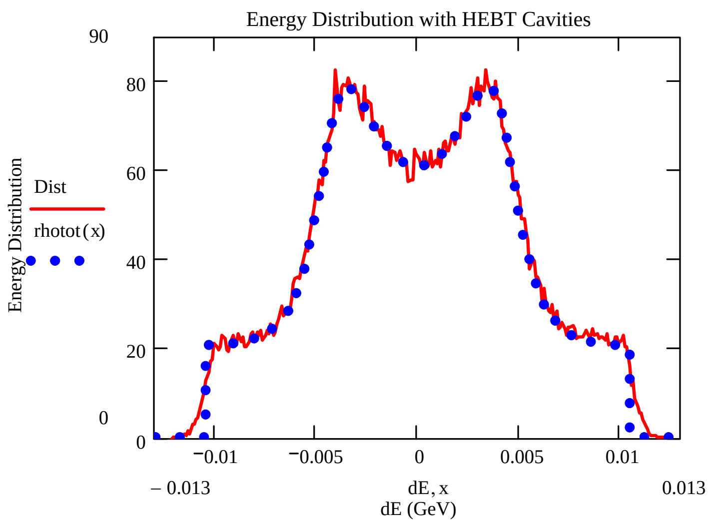

Calculation of Stability Boundaries (courtesy J. Holmes)

- Stability boundaries were calculated for the candidate functions in the usual way, using Mathcad and Mathematica.
  - The top plot is the stability boundary for the density with no EC or ES cavities, while the bottom plot is that obtained with cavities.
  - The axes correspond to imaginary (horizontal) and real (vertical) impedances, respectively.
  - The scales of the two plots are essentially the same. For n = 10 and zero chromaticity, 0.001 on either axis corresponds to 11.2 kΩ/m, while for natural chromaticity 0.001 represents 105.5 kΩ/m.
  - Space charge impedance is about 3.5 MΩ/m. It means that the stability disappears due to space charge tune shift (even for natural chromaticity)

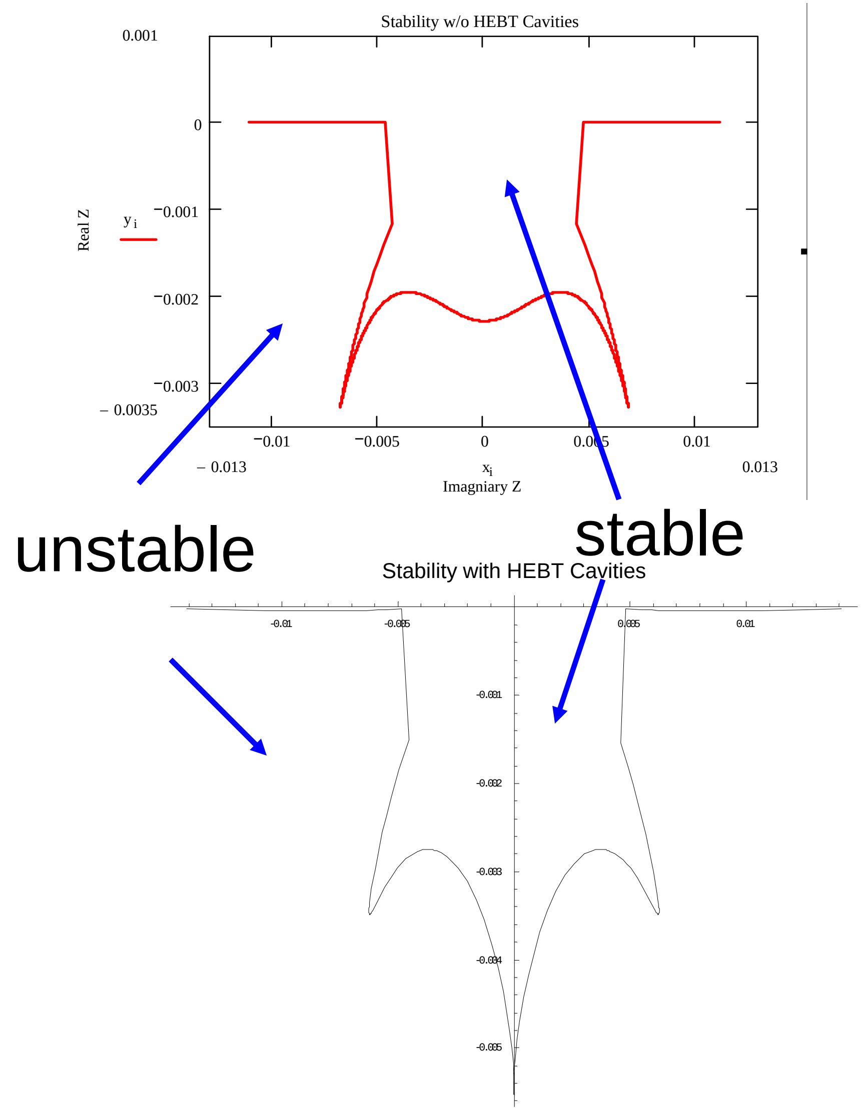

Comparison of Computational and Analytic Thresholds (courtesy J. Holmes)

In order to compare the analytic results with ORBIT predictions, we take the post-injection fully evolved beam distribution with impedance turned off, and then subject it to the given impedance. The thresholds, obtained in this way are somewhat different than would be observed in the actual machine.

Case	Analytic Result	ORBIT Result
Extraction Kicker Impedance, Bunched Beam **Natural Chromaticity, No Space Charge**	**N/A**	**N_{th} >~ 10^{15}** **Broadband peaks n ~ 10**
Extraction Kicker Impedance, Bunched Beam **Zero Chromaticity, No Space Charge**	**N/A**	**N_{th} <~ 10^{14}** **Broadband peaks n ~ 10**
Extraction Kicker Impedance, Bunched Beam **Zero Chromaticity, 3D Space Charge**	**N/A**	**N_{th}>~3×10^{14}**
n = 10, Bunched Beam, N = 1.5×10^{14} **Natural Chromaticity, No Space Charge**	**N/A**	**Ω_{th} ~ 800 k Ω/m**
n = 10, Coasting Beam, N = 1.5×10^{14} / 0.4 **Natural Chromaticity, No Space Charge**	**Ω_{th} = 241 k Ω/m**	**Ω_{th} ~ 200 k Ω/m**
n = 10, Coasting Beam, N = 1.5×10^{14} / 0.4 **Zero Chromaticity, No Space Charge**	**Ω_{th} = 25.4 k Ω/m**	**Ω_{th} ~ 25 k Ω/m**
Previous case with Lorentz distribution	**Computational and Analytic Thresholds Agree within 5%**	

Summary of Coasting Beam vs ORBIT study

- For smooth energy distributions thresholds agree within 5%
- For nonanalytic distributions (approximations for real distributions) ORBIT and analytic results agree within 20%.
- Most pronounced discrepancy – coasting beam model gives always instability for SNS ring energy distributions, while realistic simulation with 3D space charge shows the beam is stable for 3×10^{14} protons in the ring.
- Several reasons – betatron tune spread due to space charge, bunched beam spread of betatron tunes along the longitudinal coordinate due to vacuum chamber, bunched beam coupling of many modes (from ORBIT simulation bunched beam 4 times more stable in case of no space charge only real impedance), etc.
- Intermediate conclusion – real bunched beam dispersion relations has to be obtained to describe our particular SNS Ring situation

Summary

- Transverse Impedances are updated and associated instabilities are investigated
- The threshold of conventional instabilities due to extraction kicker impedance is in the region of 2 MW. The work on getting accurate threshold for the updated Extraction Kicker Impedance is in progress.
- Control knobs for instability threshold increase are partially identified (chromaticity)
- More deep analysis of instability mitigation requires development of real bunch beam stability diagrams
- First steps toward this ultimate goal (bunched beam instability description) are made – the analysis needs substantial amount of time and effort

Bunched Beam Dispersion Relations

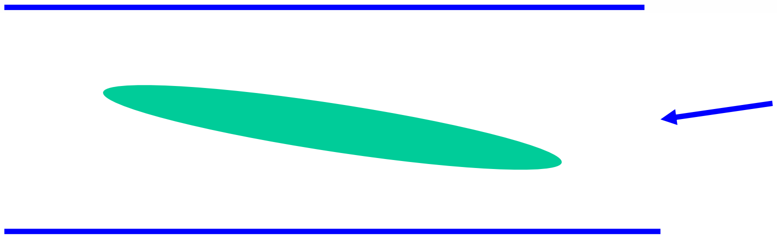

Bunched beam instabilities are mostly referred to as head-tail instabilities. The dipole moment can not be sinusoidal function of longitudinal coordinate. Synchro-betatron modes (and their coupled combinations) are used instead. In general, this instability requires mode coupling analysis of thousands of synchro-betatron modes (M. Blaskiewicz, 1998 ICFA Workshop in BNL)

Coasting beam

$$D(z,\delta,\tau) = d_s(\delta,\tau)\exp\{i(2\pi n\frac{z}{\Pi} + \omega_b t)\}$$

Bunched beam

$$D(z,\delta,\tau) = d_s(\delta,\tau,z)\exp\{i\omega_b t)\}$$

$$2i\omega_b(\frac{\partial}{\partial t}d_s + \frac{dz}{dt}\frac{\partial}{\partial z}d_s + \frac{d\delta}{dt}\frac{\partial}{\partial\delta}d_s) = \frac{F\exp(-i\omega_b t)}{\gamma m}$$

$$\chi_n = \frac{-qIZ_\perp(n\omega_0 + \omega_b)}{2\gamma m(\beta c)^2}\beta_{s_0}$$

$$= 0$$

$$= U_0 \sin\frac{z}{\lambda}$$

$$\Delta(\delta) = \frac{\eta\delta}{\beta^2}2\pi\left|n + \nu_b + \xi\right|$$

Collective Equations to Solve

$$\frac{\partial d_s(\delta,\tau)}{\partial\tau} + i\Delta(\delta)d_s(\delta,\tau) = \chi_n\int_{-\infty}^{\infty}g(\delta)d_s(\delta,\tau)d\delta$$

$$\frac{\partial d_s(\delta,\tau,z)}{\partial\tau} + \frac{C\eta\delta}{\beta^2}\frac{\partial d_s(\delta,\tau,z)}{\partial z} - \frac{U_0 z}{\lambda}\frac{\partial d_s(\delta,\tau,z)}{\partial\delta}$$

$$= -\sum_{n=-\infty}^{\infty}\chi_n\int_{-\infty}^{\infty}\oint g(\delta)d_s(\delta,\tau,z')\exp(-\frac{i2\pi n(z'-z)}{C})d\delta dz'$$

Ultimate Goal – to Get Solution for This

How it Is Possible to Analyze/Solve It?

- Simplifying the model – removing nonlinearity of space charge force first (i.e. using self-consistent 3D distributions with linear space charge force)
- Assuming number of large harmonic in Impedance is small
- Finding solution for initial conditions instead of finding eigen modes of the problem. This is similar to Landau solution to the problem. Contrary to Landau approach, eigen modes approach leads to so-called Van Kampen singular modes analysis, which is not important for stability.
- Using all the above, we obtained first dispersion diagram for one single harmonic of the impedance and see how it can be expanded to few harmonic analysis (needs substantial time and effort to make good investigation on this).
- Our feeling is that only on this way we can make "fast assessment of Landau damping, and it could guide strategies for beam stabilization, e.g. by adjusting chromaticity, nonlinearities, coupling, or the painting scheme".

Magnet Analysis and Engineering Support

D. Raparia
SNS/BNL

Sept 27-29, 2004

TiN coating of extraction kicker ferrite modules (Hseuh , Lanfa …)

Purpose: To reduce secondary electron emission from ferrite (and Cu) surface, suppress multipacting

Goal: 0.1 μm TiN on ≥ 90% inner surface, with good adhesion

AP Calculations: Eddy current & heating, E-M smoothing...
(Aleksandrov, 12/00', Blaskiewicz, 12/01')
i.e strips of 1 cm wide: ΔT ~ °C, ΔP ~ watts, Δt ~ ns

Effectiveness of electron suppression with 90% coating

un-coated, λ_{peak}=200nc/m
100% coated, λ_{peak}=10nc/m
90% coated, λpeak=20nc/m
80% coated, λ_{peak}=33nc/m
70% coated, λpeak=50nc/m

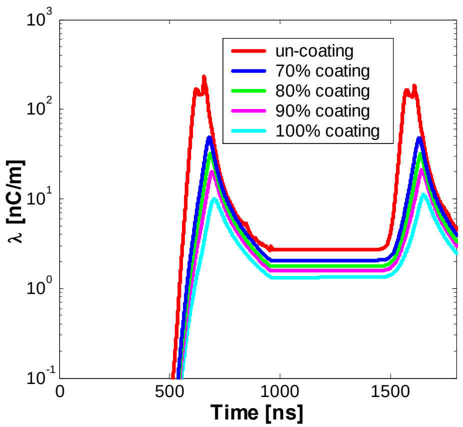

Two turns shown

Coating: developed using kicker test chamber and prototype kicker

Coating strips of 1cm (Y) x 5cm (Z) with 1mm gaps using custom masks

Good adhesion;

Resistance across strips > 100 Ohm;

E-M smoothing time of < 1 ns (Blaskiewicz, 4/04'); may be reduced with improved masking or scraping after coating

SEY in Un-coated ferrite area 2.5

SEY in ferrite area coated with TiN 1.9

Un-coated area: Tall 20%, short 30%

TiN coating effect on Impedance

(H. Hahn et al)

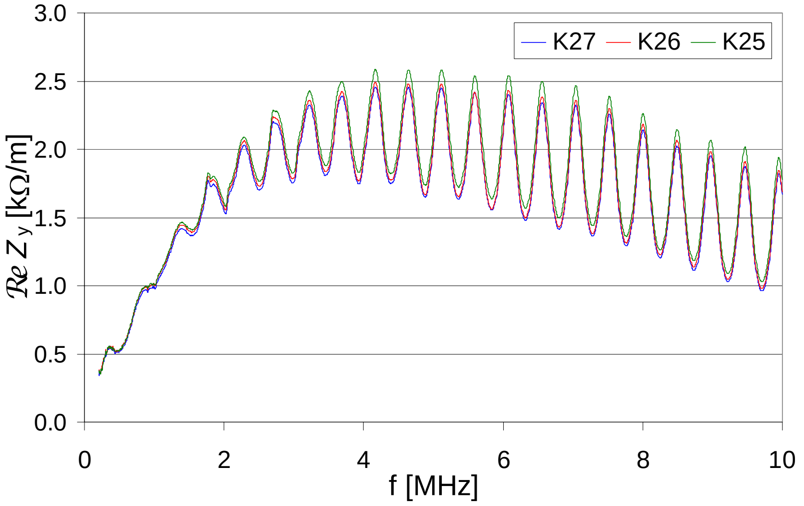

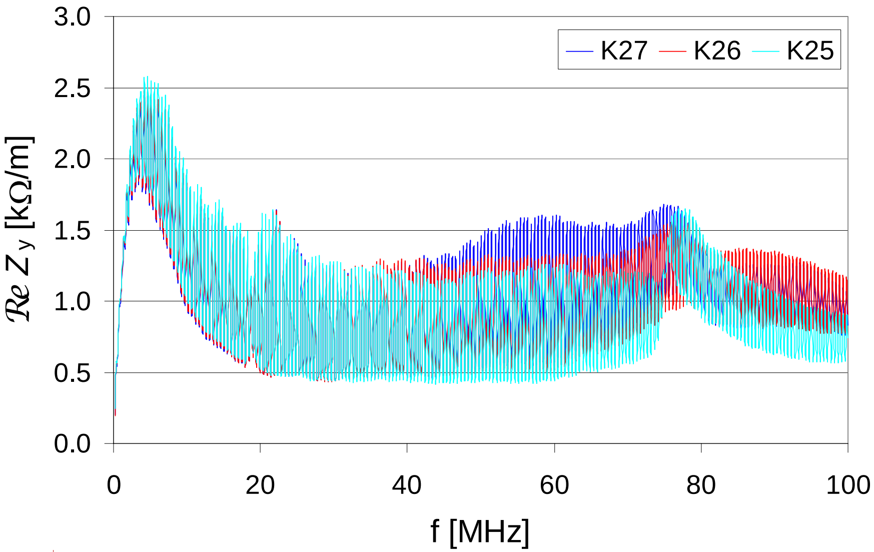

Three Kicker module were measured
K25, K26 K27
24.3 cm 15.1 cm 39 cm
(prototype (24.3, 15.9, 36)

K26 was coated with TiN
3 magnets in 3.8 m Long production Vessel

No effect of TiN coating seen

Backscatter electron yield

(Lanfa …)

Electron yield of CARBON is about one order-of-magnitude smaller that that of Copper at the energy 525keV

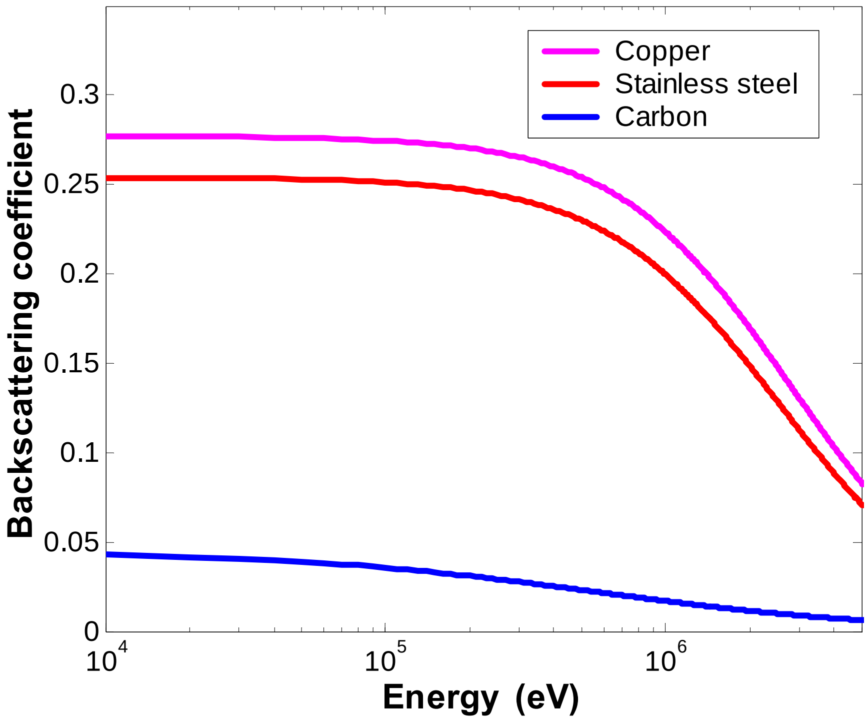

Electron yield with of monoenergetic electrons impinging normally on the thick Copper, stainless steel, and Carbon

Stripped electron spatial distribution

(Lanfa …)

foil center(40,23,307)

Bfield at foil center=(-3.6,2504,-547.9)Gauss, α=210mrad

E=522keV, B=2500G, ρ=11.98mm, T=0.289ns, v=2.6e8m/s, β=0.866, γ=2

Catcher shape: β=25°, θ=65°

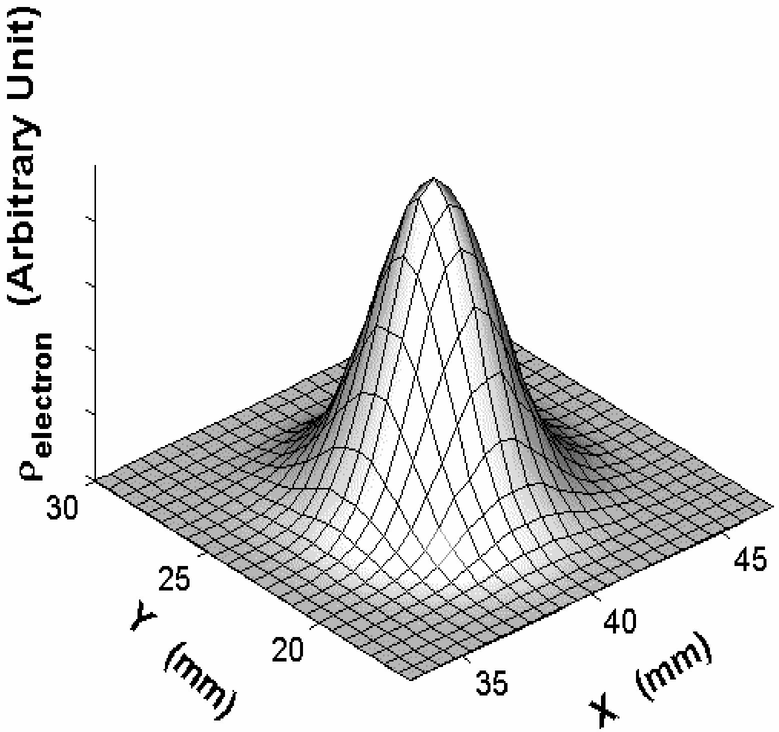

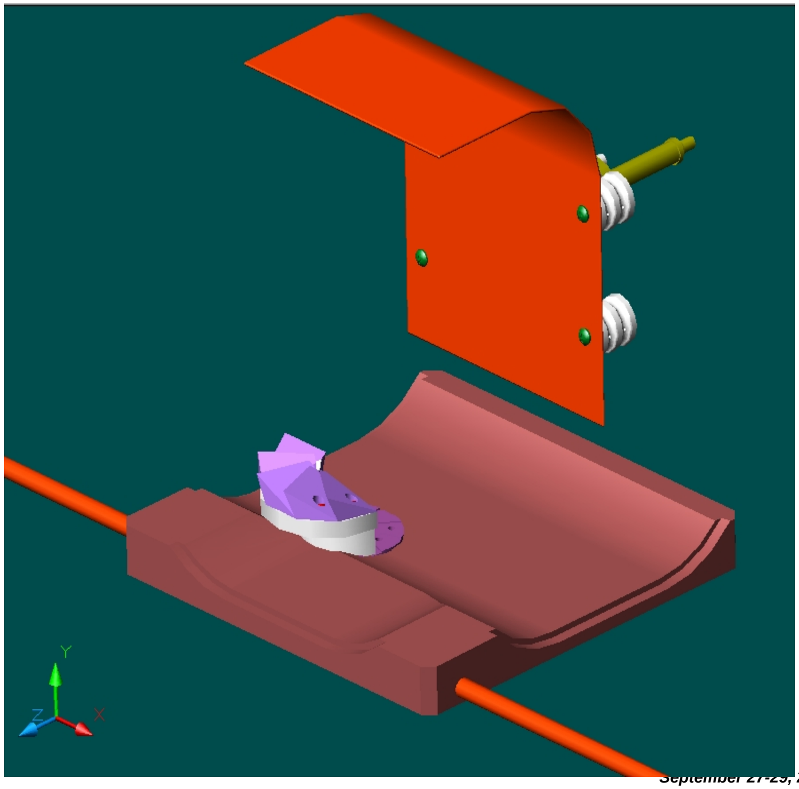

Orbits of electron

(Lanfa …)

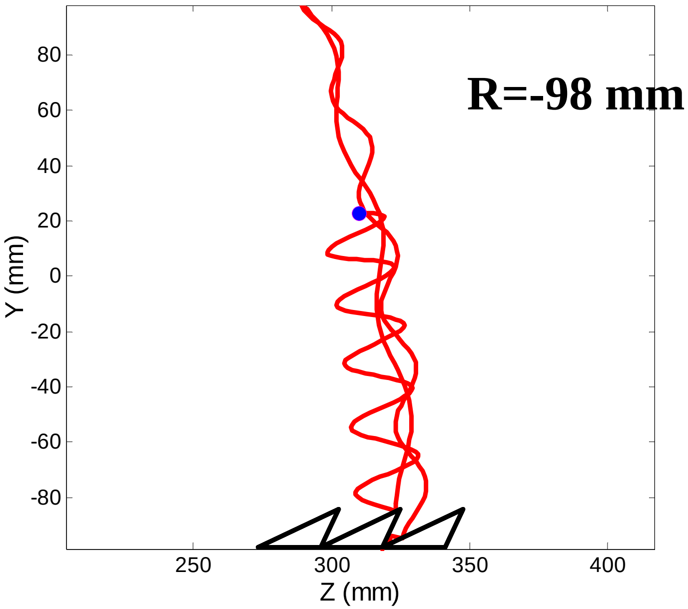

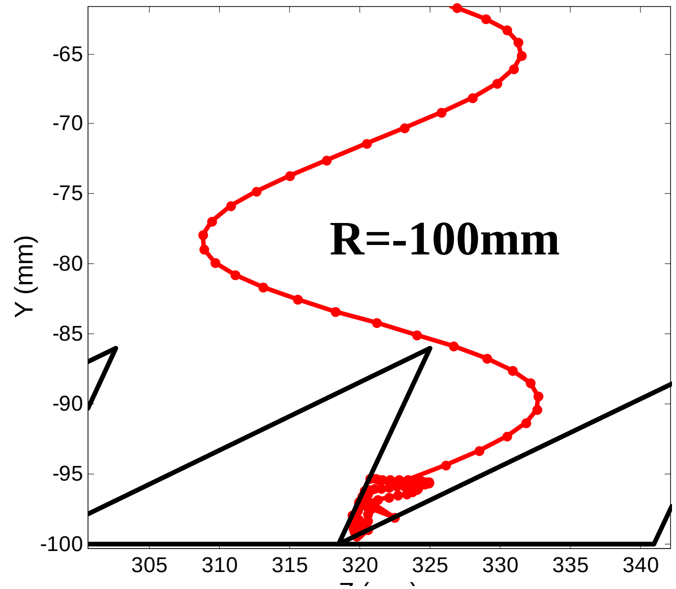

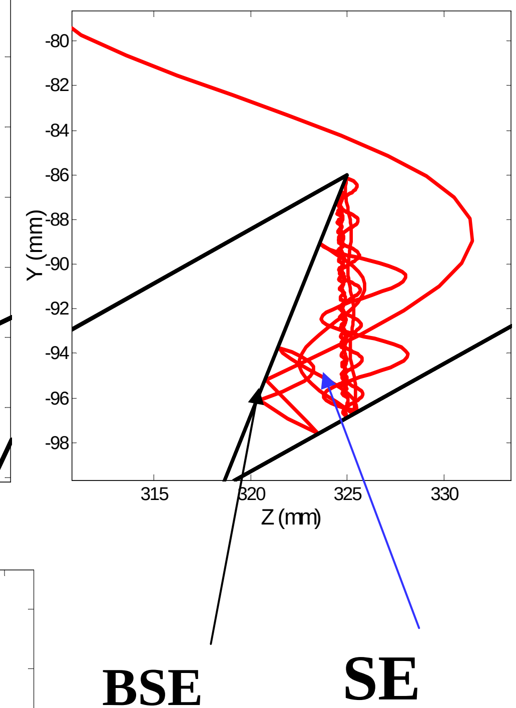

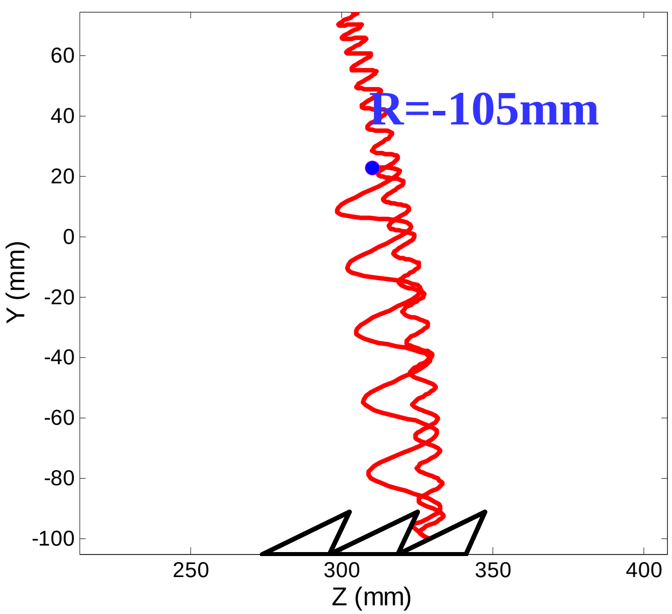

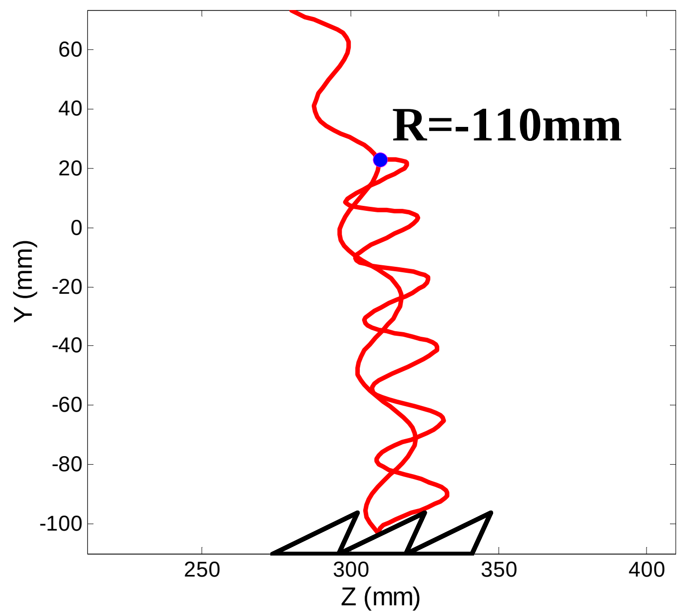

Secondary electrons have less change of turning back to the foil than the backscatter electrons

Distribution of electrons

(Lanfa …)

- **100% stripped electrons first hit the front plane of the catcher within small region: ΔX=10 mm, ΔY=5 mm, ΔZ=2 mm**

- **The result is sensitive to the catcher's position**

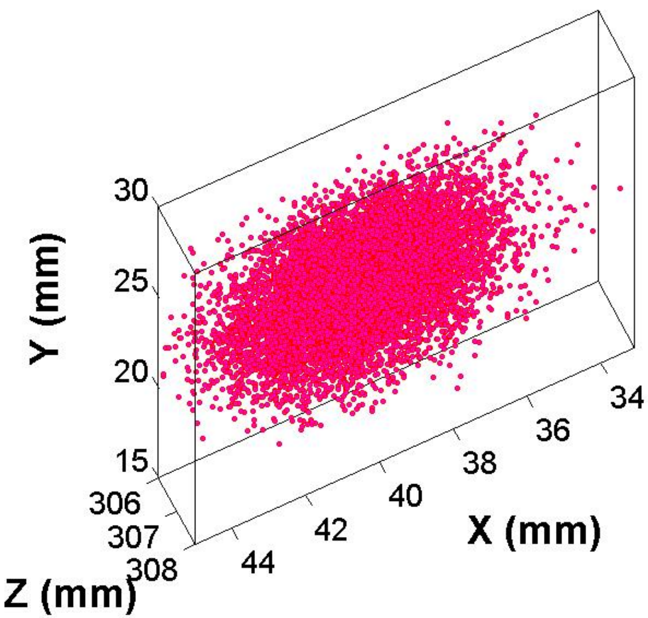

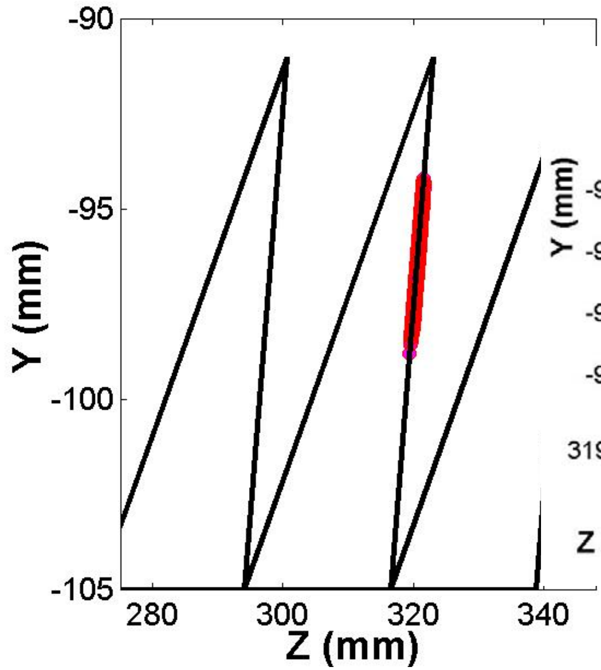

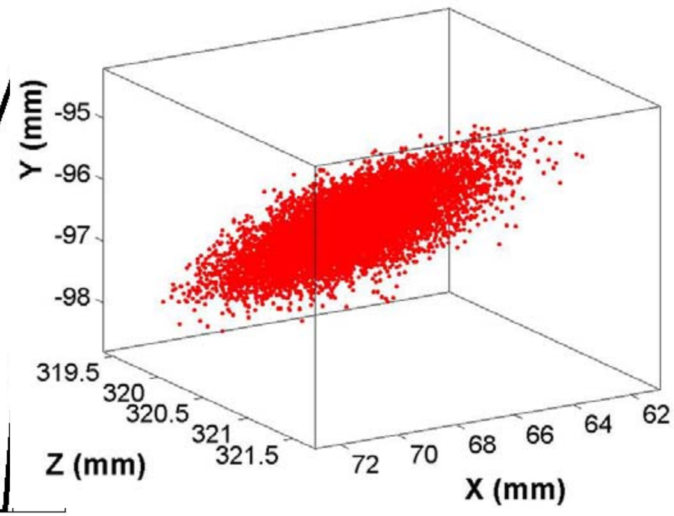

Distribution of the stripped electrons

Distribution of the electrons when they hit the catcher

$\Delta Z=2$ mm $\Delta\theta_{z_xy}=2$mrad

ΔX=10 mm, ΔY=5 mm, ΔZ=2 mm

Electron distribution with carbon catcher

- There is no multipacting due to the low electron yield
- There are 0.34% backscattered electrons;
- Secondary electrons are confined

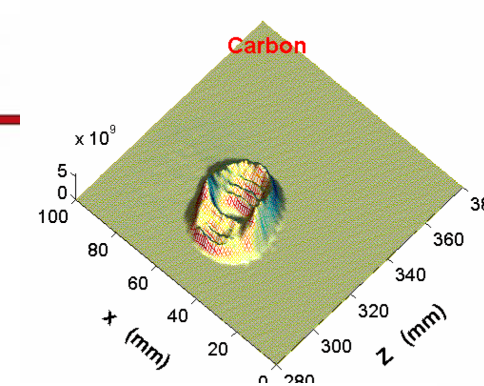

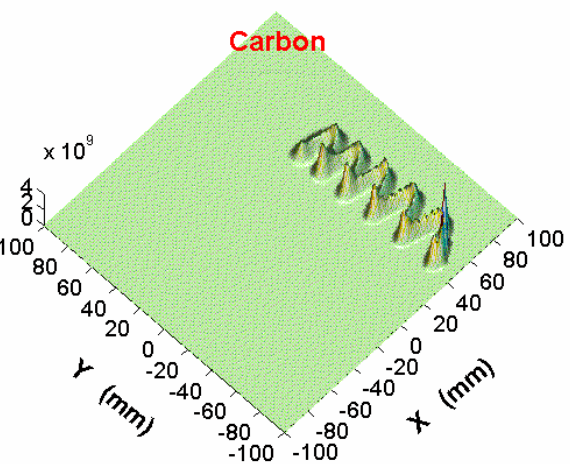

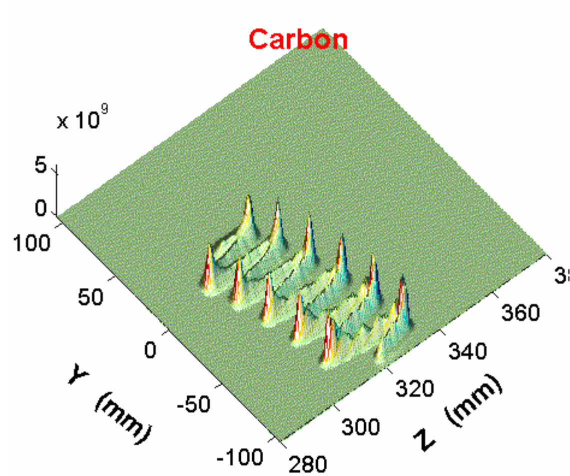

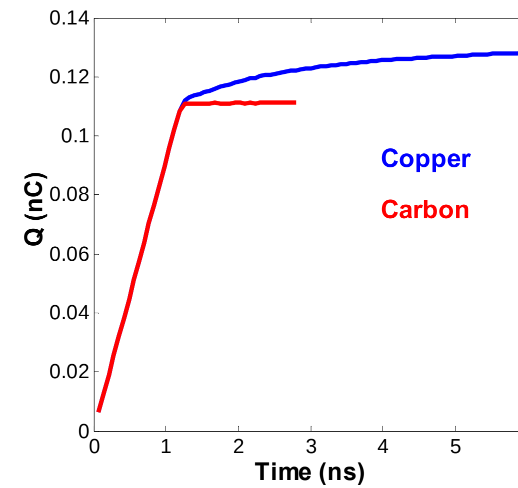

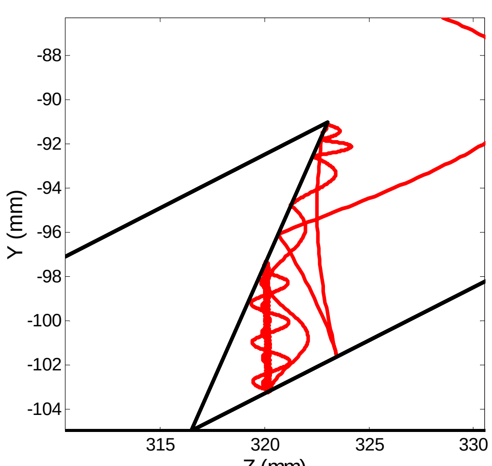

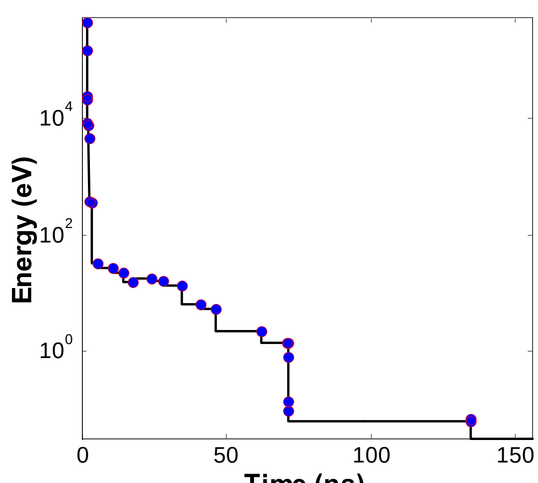

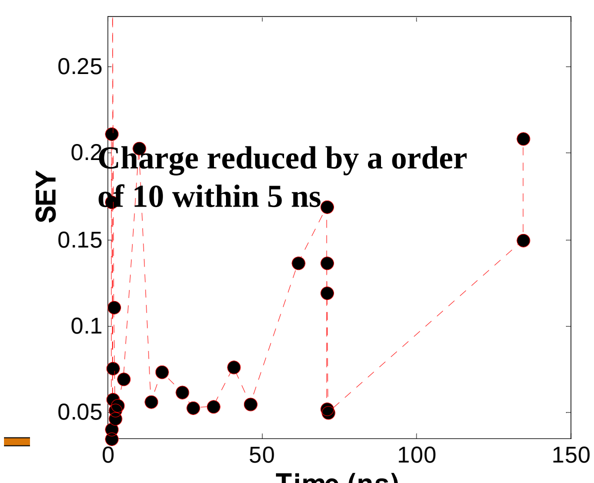

Charge reduced by a order of 10 within 5 ns

Copper catcher
(Lanfa …)

- Electron saturated within a few ns (~5ns)
- There is no multipacting due to the low electron yield
- There are 7.8% backscattered electrons

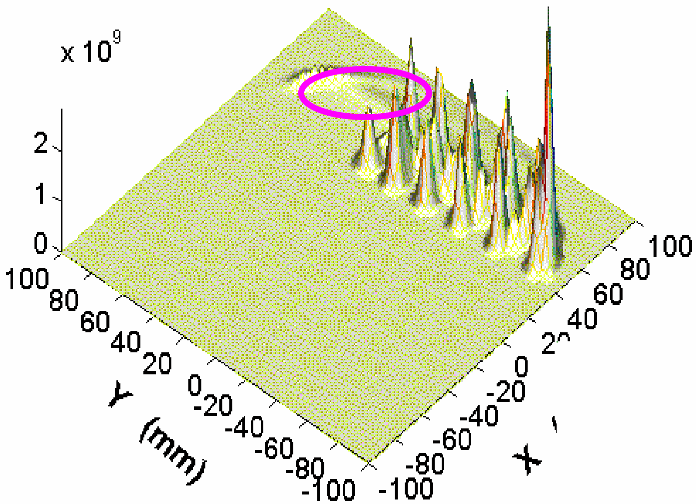

Backscattered electrons

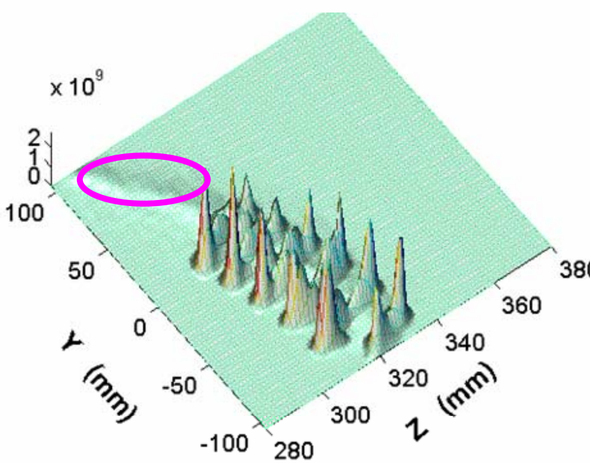

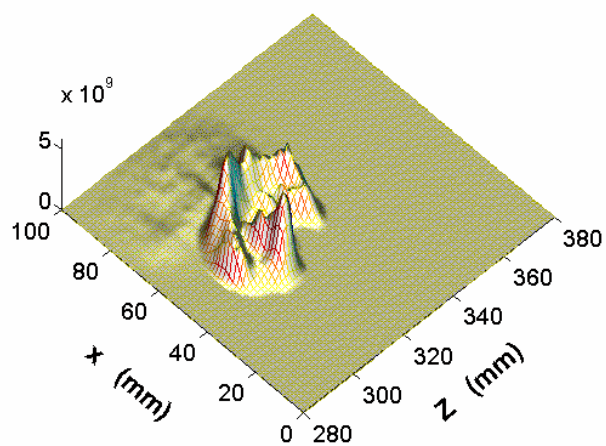

Studies to be completed

-Injection

- Electron Density + Protons
- Electron Density + Electrode
- Electron Density + Electrode +Proton

-BPM

-Collimator

ORBIT Benchmark of Montague Resonance Crossing in CERN PS (Cousineau, Holmes)

Experimental Data:

- Emittance measured in the CERN PS while passing through Montague resonance.
- Fixed ν_y (ν_y=6.21), vary ν_x (ν_x = 6.15 $\rightarrow$ 6.25).

Benchmark results:

- Real CERN PS lattice is modeled
- Result in good agreement; ORBIT reproduces experimentally-observed asymmetry in stopband; predicts slightly larger stopband width

Ongoing work:

- Currently performing cross-code benchmark with IMPACT code for ring.
- Investigating effects of lattice and dispersion.

Collaboration with E. Metral, I. Hofmann, R. Ryne, J. Qiang

Red: Horizontal

Blue: Vertical

Points (data), Lines (simulation)

Emittance exchange in Montague resonance

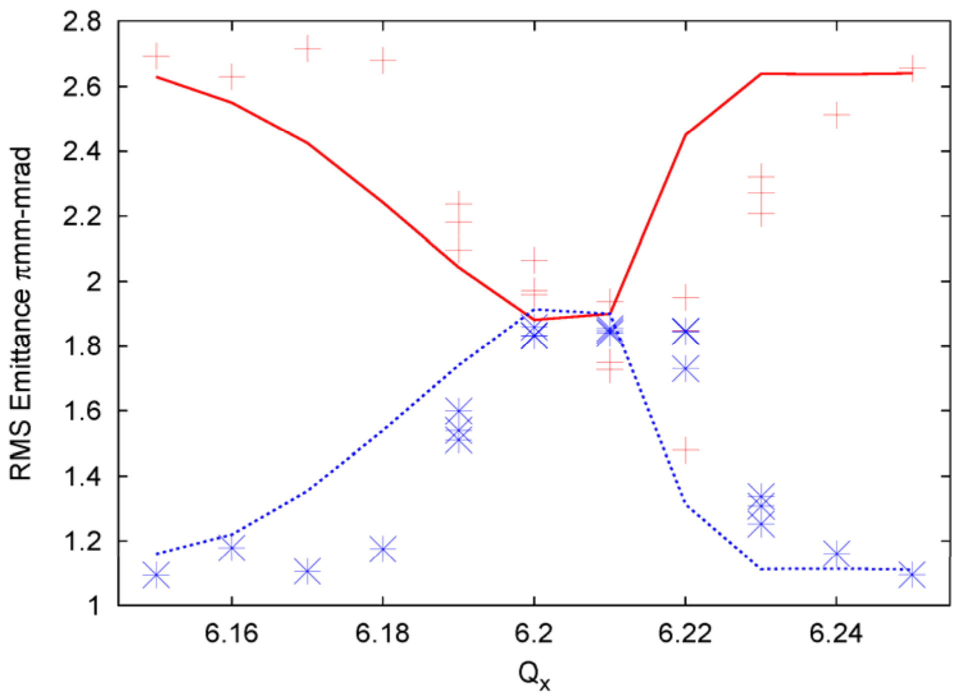

For Comparison: IMPACT Simulations of Montague Resonance Crossing in CERN PS (dashed lines)

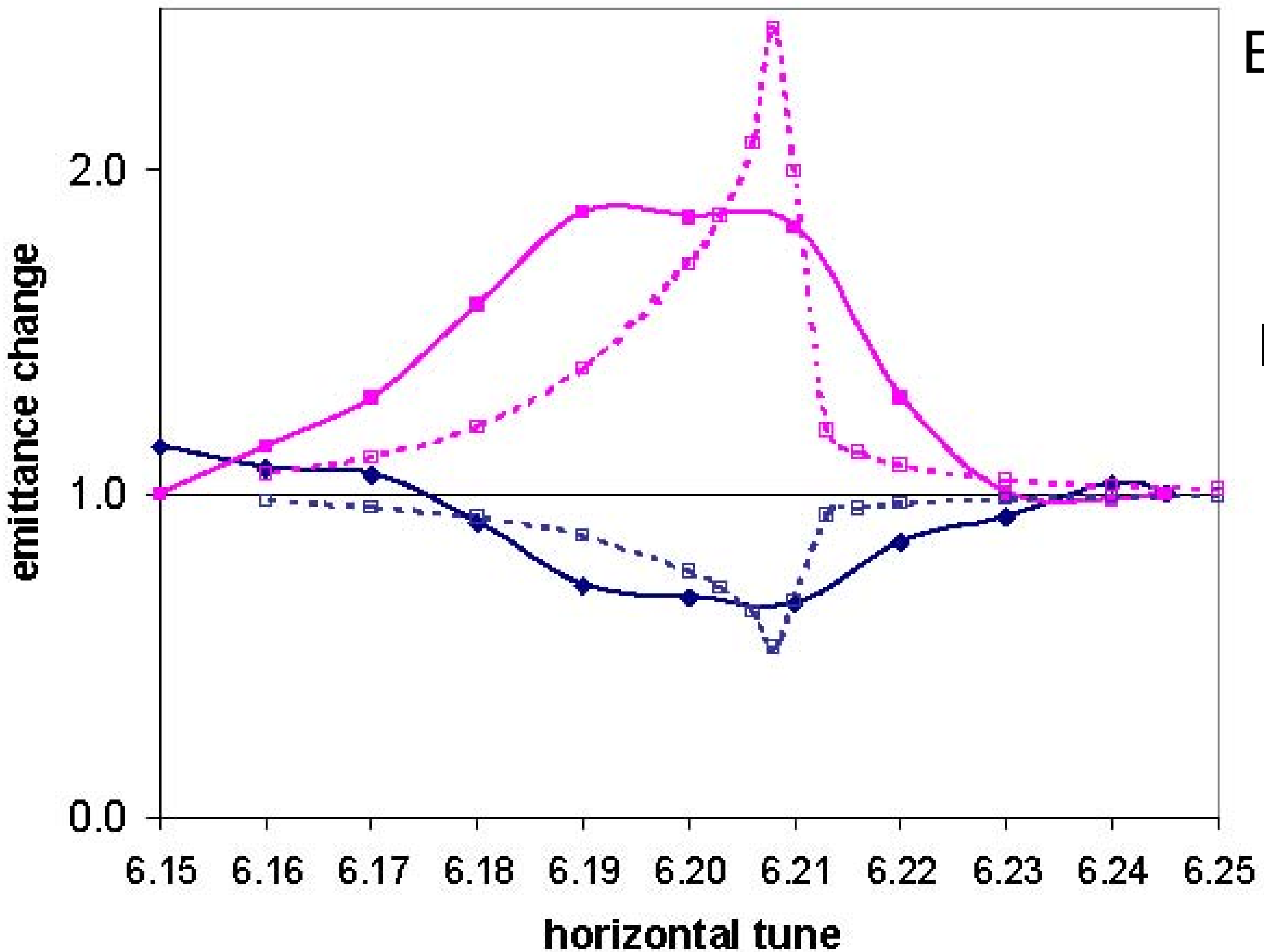

E. Metral et al., EPAC'04, Simulations by IMPACT code

Expected scope & budget changes

- Remaining two magnets & RTBT shielding suffering from high steel prices
  - "Worldwide (China boom) and Domestic (Humvee armor plate) steel shortage as resulted in significant cost increases for magnet cores, structural steel, and collimator shielding this year."